

## Surface Damage on Si Substrates Caused by Reactive Sputter Etching

Norikuni YABUMOTO, Masaharu OSHIMA,  
Osamu MICHIKAMI and Shizuka YOSHII

*Musashino Electrical Communication Laboratories,  
Nippon Telegraph and Telephone Public Corporation,  
Musashino-shi, Tokyo 180*

(Received February 4, 1980; accepted for publication February 21, 1981)

Surface damage on silicon substrates caused by RSE has been investigated. Defects are classified into four categories in order of destruction, namely, precipitates surrounded by elastic strain field, surface roughness pattern, polycrystalline and amorphous silicon, and no defects, based on the results of TEM and RHEED observation. In particular, precipitates which reach a depth more than 500 Å were found to cause OSF. The surface damage consists of contamination (C, F, O) layer, C and defect mixed layer, and defect layer in order from the top. The degree of these defects and contaminations expand with increasing power density and etching duration. RSE conditions, where no defects are formed, were determined, *e.g.*, within 1 minute at  $0.4 \text{ W cm}^{-2}$ .

### §1. Introduction

Dry etching for semiconductor device fabrication has been developed to realize fine line resolution, cleanliness, low-cost and process brevity.<sup>1)</sup> Reactive sputter etching (RSE), using RF sputtering configuration, is effective for the selective etching of  $\text{Al}^{2)}$  and  $\text{SiO}_2$ <sup>3)</sup>, while plasma etching is used to remove polycrystalline Si and  $\text{Si}_3\text{N}_4$  films. Since RSE is suitable for good pattern delineation,<sup>4)</sup> this method will be adopted for all dry etching process.

RSE utilizes not only the chemical effects of reactive ions but also the physical effects of ion bombardment.<sup>5)</sup> The radiation damage thickness at silicon substrate surface, caused by  $\text{Ar}^+$  ion bombardment during ion etching of  $\text{SiO}_2$  films at energy below 1 keV, is 50–100 Å.<sup>6)</sup> In the case of RSE, ions ( $\text{CF}_x^+$ ,  $\text{CCl}_x^+$ ) also impinge on the surface at several hundreds of eV, therefore surface damage may be formed. Damage is expected to consist of defects due to ion bombardment and contaminations due to decomposed etching gas, and can be cause of electrical characteristic deterioration. However, very few studies on surface damage caused by RSE have been reported.

In the present paper, the surface damaged layer on silicon substrates caused by over-etching of RSE after removal of  $\text{SiO}_2$  films

tron microscopy (TEM), reflection high energy electron diffraction (RHEED), oxidation Sirtl (OS) check and Auger electron spectroscopy (AES). Based on the obtained results, the recommended RSE conditions where no defects were formed on silicon substrates were proposed.

### §2. Experimental Procedures

Experiments were carried out using a diode RF sputter etching apparatus with a 100 mm $\phi$  target. The (100) and (110) surface silicon wafers with no  $\text{SiO}_2$  films were reactive-sputter-etched. Then, crystal structures and contaminations in the surface damaged layer were investigated by TEM, RHEED, OS check and AES. Since etching gas, gas pressure, power density, etching duration and target materials were considered to influence the surface damage, RSE conditions were set as shown in Table I.  $\text{C}_2\text{F}_6$  gas was used as etching gas, because active species for  $\text{SiO}_2$  were  $\text{CF}_3^+$  ions<sup>7)</sup> and  $\text{C}_2\text{F}_6$  gives more  $\text{CF}_3^+$  ions, compared with  $\text{CF}_4$ .<sup>8)</sup> Ar,  $\text{C}_2\text{H}_4$  and  $\text{O}_2$ , respectively, were mixed with  $\text{C}_2\text{F}_6$  in order to extract sputtering effects, increase etching selectivity for  $\text{SiO}_2/\text{Si}$ <sup>9)</sup> and make faster etch rate by raising chemical effects.<sup>10)</sup> Gas pressure was set at 0.04 Torr. Power densities were set from 0.13 to  $1.3 \text{ W cm}^{-2}$ . Etching durations were 5 seconds to 5 minutes. The target placed on

Table I. RSE conditions.

Etching gas	Pressure [Torr]	Power Density [ $\text{W cm}^{-2}$ ]	Etching duration [sec]
$\text{C}_2\text{F}_6$	0.04	0.13, 0.25, 0.6, 1.0, 1.3	5, 15, 30, 60, 120, 180, 300
$\text{C}_2\text{F}_6 + \text{Ar}$	0.04	1.0	300
$\text{C}_2\text{F}_6 + \text{C}_2\text{H}_4$	0.04	1.0	180
$\text{C}_2\text{F}_6 + \text{O}_2$	0.04	1.0	180

the lower electrode was a carbon plate. Although iron and teflon plates were also used as targets, no particular difference in surface damage could be recognized.

Samples for TEM observation were prepared by RSE of silicon thin films, which were made by conventional thinning technique using  $\text{HF} + \text{HNO}_3 + \text{CH}_3\text{COOH}$  solution, as shown in Fig. 1. The same surface damage was observed on the substrates regardless of the samples used. One was made by chemical back etching after RSE of silicon wafer. The other was ready for RSE of silicon thin film.

### §3. Results and Discussion

Defects on silicon substrates caused by RSE are described in §3.1. Section 3.2 deals with gas mixing effects on defects and §3.3 with OS check results. Section 3.4 describes contamination in surface damaged layer. Finally RSE conditions are discussed in §3.5.

#### 3.1 Defects caused by RSE

The dependence of surface damage structure on etching conditions, that is, power density, etching duration,  $\text{C}_2\text{F}_6$  pressure and target materials, was investigated. The defects formed in RSE for long duration at high power density were found by TEM observation to be precipitates surrounded by elastic strain field. They existed on  $\{111\}$  planes along  $\langle 011 \rangle$  directions taken from (100) direction, as shown in Fig. 2(a). These defects proved to be formed on silicon substrates regardless of gas pressure and target materials. Figure 3(a) shows the defects which were formed using  $\text{CF}_4$  gas and iron target at 0.04 Torr. Figure 3(b) shows the defects formed using  $\text{C}_2\text{F}_6$  gas and teflon target at 0.1 Torr. On the other hand, surface roughness pattern was formed under RSE conditions at lower power density, as shown in Fig. 2(b). In these cases no defects were observed on the TEM samples without RSE.

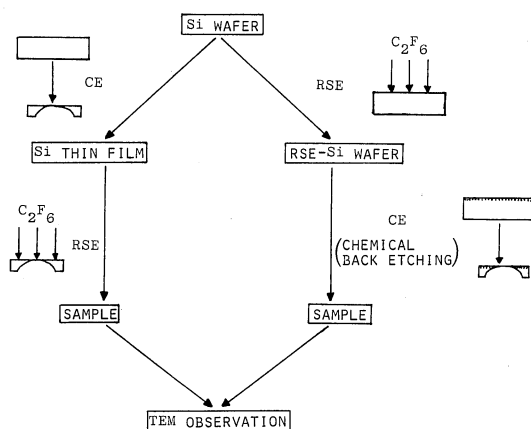


Fig. 1. TEM observation samples.

structure depends especially on power density and etching duration. Then, the dependence of damage structure on these parameters was investigated by TEM at a  $\text{C}_2\text{F}_6$  pressure of 0.04 Torr with a carbon target. The tendency of damage formation conditions is summarized as follows. (1) Precipitates surrounded by elastic strain field are formed with RSE for more than 1 minute at more than  $1 \text{ W cm}^{-2}$ . (2) No defects are observed within 15 seconds at  $1 \text{ W cm}^{-2}$  or within 5 minutes at  $0.25 \text{ W cm}^{-2}$ . (3) Surface roughness pattern is formed under intermediate conditions. Figures 2(a)–(c) show typical TEM images of these defects. More detailed results will be described in §3.5 using Fig. 13 which will be drawn up based on RHEED observation and OS check in addition to TEM observation.

Since precipitates existed on  $\{111\}$  planes, (110) surface silicon films were used in order to make clear TEM image. Figure 4 shows a dark field TEM image of this defect using (222) spot. This defect proved to be interstitial type inclusion, because the image changed from light to dark before and behind the defect along the direction of reciprocal lattice vector.<sup>11)</sup>

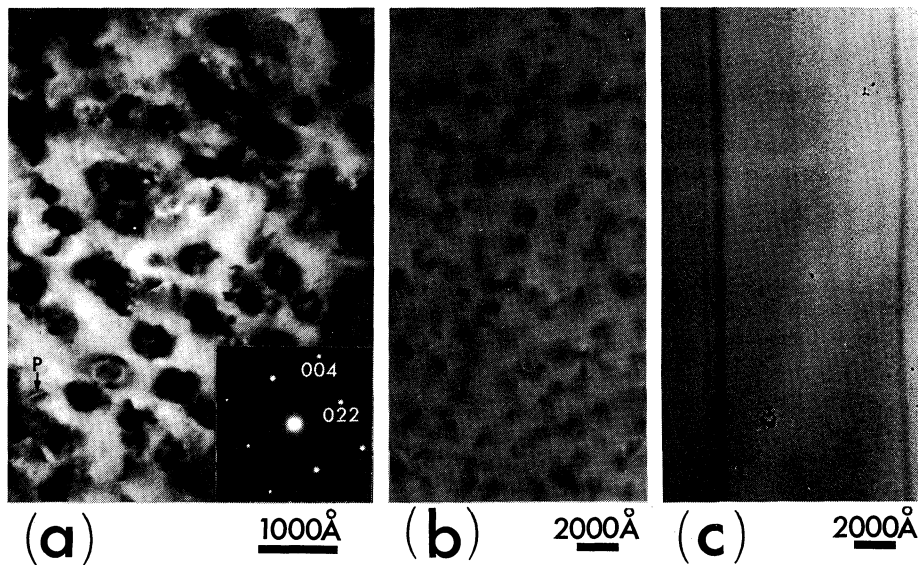


Fig. 2. TEM bright field images of (100) silicon films: (a) Precipitates surrounded by elastic strain field, RSE for 3 minutes at  $1 \text{ W cm}^{-2}$ . P shows a precipitate. (b) Surface roughness pattern, RSE for 3 minutes at  $0.6 \text{ W cm}^{-2}$ . (c) No defects, RSE for 3 minutes at  $0.25 \text{ W cm}^{-2}$ .

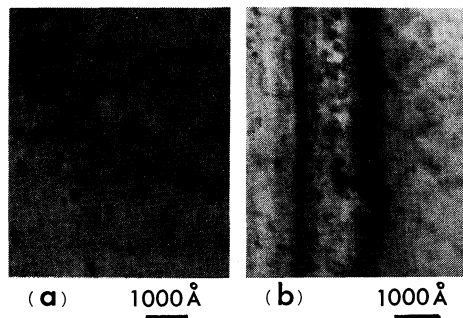


Fig. 3. TEM bright field images of surface damage under various RSE conditions: (a)  $\text{CF}_4$ , 0.04 Torr,  $1.3 \text{ W cm}^{-2}$ , 3 min, iron target. (b)  $\text{C}_2\text{F}_6$ , 0.1 Torr,  $1.3 \text{ W cm}^{-2}$ , 3 min, teflon target.

that the region containing these defects remains single crystal. Then, the damage structure in the extreme surface region was investigated by means of RHEED. The observation was carried out at a pressure of  $10^{-6}$  Torr and with an accelerating voltage of 200 kV. Samples were washed with HF solution and rinsed with  $\text{H}_2\text{O}$  after RSE. After this treatment, carbon contaminations on the surface was washed away, which was ascertained by AES analysis.

Figures 5(a)–(d) show RHEED patterns of reactive-sputter-etched (110) silicon surface. Under RSE conditions where precipitates and surface roughness pattern were observed,

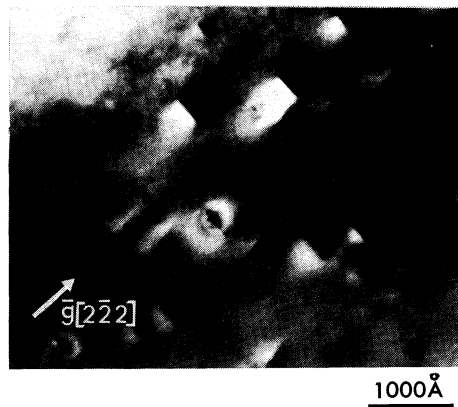


Fig. 4. TEM dark field image of (110) silicon film using  $(\bar{2}\bar{2}\bar{2})$  spot. RSE for 3 minute at  $1 \text{ W cm}^{-2}$ .

phous silicon halo pattern occurred, as shown in Fig. 5(a) and (b). Even under RSE conditions where no defects were observed by TEM, a small amount of polycrystalline silicon was formed, as shown in Fig. 5(c). The strongest polycrystalline silicon ring pattern occurred at  $0.6 \text{ W cm}^{-2}$ . Over  $0.6 \text{ W cm}^{-2}$ , the amorphous silicon halo pattern grew stronger and the polycrystalline ring pattern became weaker. The single crystal silicon rod pattern changed to a round, ring and halo pattern with increasing power density and etching duration, which indicates that the substrate surface became

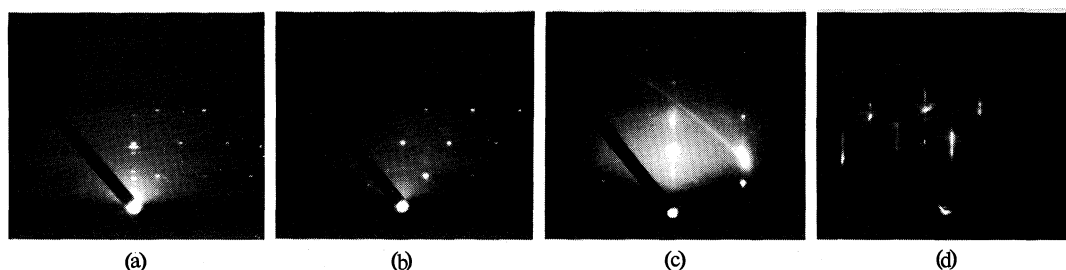


Fig. 5. RHEED patterns of reactive-sputter-etched (110) silicon wafers: (a) RSE for 3 minutes at  $1 \text{ W cm}^{-2}$ . (b) RSE for 3 minutes at  $0.6 \text{ W cm}^{-2}$ . (c) RSE for 3 minutes at  $0.25 \text{ W cm}^{-2}$ . (d) RSE for 3 minutes at  $0.13 \text{ W cm}^{-2}$ .

destroyed. In etching for 1 minute at  $0.25 \text{ W cm}^{-2}$  or up to 5 minutes at  $0.13 \text{ W cm}^{-2}$ , no defects were observed.

### 3.2 Gas-mixing effects on surface damage

RSE is a technique to etch materials both by sputtering effects and by chemical effects. Then, Ar,  $\text{C}_2\text{H}_4$  and  $\text{O}_2$  gases were added to  $\text{C}_2\text{F}_6$  in order to investigate the influence of the two effects on surface damage. Figures 6(a)–(d) show the dependence of surface damage on Ar ratio in the Ar +  $\text{C}_2\text{F}_6$  mixed gas. The surface destruction enlarged with increasing the Ar ratio, that is, ring patterns appeared in addition to the single crystal silicon (100) pattern in selected area electron diffraction. They correspond, as shown in Table II, to polycrystalline silicon and  $\beta$ -silicon carbide (zinc blende type). Polycrystallization of silicon substrate surface is enhanced with increasing Ar sputtering effects, while polycrystalline silicon was ob-

served only by RHEED on the silicon surface etched with the pure  $\text{C}_2\text{F}_6$ . Therefore, the polycrystallization is thought to be taken place by ion bombardment effects. In the case of  $\text{C}_2\text{F}_6$ , the momentum given to the surface by  $\text{CF}_x^+$  ions could be consumed in the chemical reaction. Accordingly, the ion bombardment

Table II. Spacing of lattice planes for polycrystalline Si and  $\beta$ -SiC in the experiment and ASTM card.

	ASTM card			Experiment		Error [%]
	d [Å]	I/I <sub>0</sub>	hkl	d [Å]	Intensity	
Si	3.14	100	111	3.21	s <sup>a</sup>	+2.2
	1.92	60	220	2.02	w <sup>b</sup>	+5.2
	1.64	35	311	1.67	m <sup>c</sup>	+1.8
$\beta$ -SiC	2.51	100	111	2.48	s	-1.2
	2.17	20	200	2.17	m	0.0
	1.54	63	220	1.48	w	-3.9
	1.31	50	311	1.34	w	+2.3

<sup>a</sup>Strong, <sup>b</sup>Weak, <sup>c</sup>Medium.

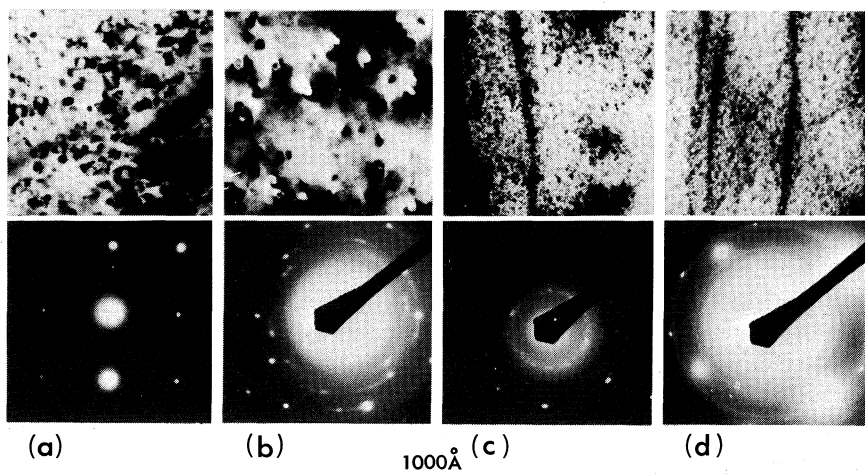


Fig. 6. TEM images and their selected area diffraction patterns of (100) silicon films using  $\text{C}_2\text{F}_6 + \text{Ar}$  mixed gas. RSE for 5 minutes at  $1 \text{ W cm}^{-2}$ : (a)  $\text{C}_2\text{F}_6 + \text{Ar}(0\%)$ . (b)  $\text{C}_2\text{F}_6 +$

effects would be reduced comparing with the case of Ar ion etching.  $\text{SF}_6$  gas is considered to have larger momentum than  $\text{C}_2\text{F}_6$ , because the ion species would be  $\text{SF}_y^+$  which has a larger mass number than  $\text{CF}_x^+$ . The experimental result shown in Fig. 7 that the similar damage to Fig. 6(d) was observed on the substrate etched with  $\text{SF}_6$  consists with the above explanation. Thus, the defects caused by RSE are found to be determined by the balance between the ion momentum and the chemical reactivity of ions.

Next,  $\text{C}_2\text{H}_4$  and  $\text{O}_2$ , respectively, were added to  $\text{C}_2\text{F}_6$  in order to increase the etching selectivity of  $\text{SiO}_2/\text{Si}$  and the etching rate of Si. In these cases, no gas-mixing effects on the defect could be observed either in the TEM

images or in the selected area electron diffractions. This is explained as follows. When  $\text{C}_2\text{H}_4$  is mixed with  $\text{C}_2\text{F}_6$ , chemical effects are reduced with decreasing free fluorine radicals. However,  $\text{CF}_x^+$  would be still an attacked species on the substrates and the degree of defects would not be enlarged. When  $\text{O}_2$  is mixed with  $\text{C}_2\text{F}_6$ , new fragment  $\text{COF}_x$  which has more momentum than  $\text{CF}_x^+$  may be formed. In this case, since chemical effects would be also increased, the degree of defects would not be enlarged.

### 3.3 Defect enhancement by thermal oxidation

OS check was carried out in order to investigate changes in the RSE-induced defects through device fabrication processes, especially thermal oxidation. Silicon wafers were reactive-sputter-etched under the conditions at which precipitates, surface roughness pattern, polycrystalline and amorphous silicon, and no defects were, respectively, formed. Then, they were oxidized at  $1100^\circ\text{C}$  for 2 hours in wet  $\text{O}_2$ . After oxide film was removed by the HF solution, the silicon surface was etched in a Wright etch solution for 1 minute. Figures 8(a) to (c) show oxidation induced stacking faults (OSF) and etch pits on the silicon surface. The relationship among OSF density, etch pit density and RSE conditions is shown in Table III.  $10^5 \text{ cm}^{-2}$  OSF were observed under the condi-

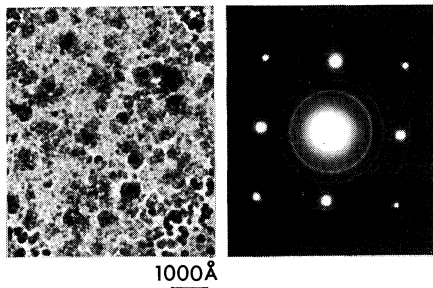


Fig. 7. TEM image and selected area diffraction pattern of (100) silicon film using  $\text{SF}_6$  gas. RSE for 3 minutes at  $1.3 \text{ W cm}^{-2}$ .

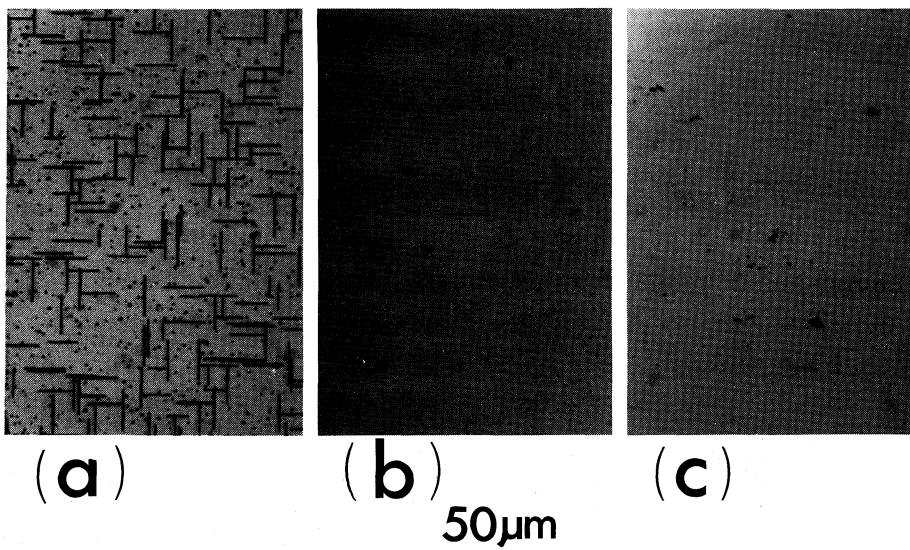


Fig. 8. Optical micrograph of (100) silicon wafers etched by Wright solution for 1 minute after thermal oxidation: (a) RSE for 3 minutes at  $1 \text{ W cm}^{-2}$ . (b) RSE for 3 minutes at

# Explore Litigation Insights

Docket Alarm provides insights to develop a more informed litigation strategy and the peace of mind of knowing you're on top of things.

## Real-Time Litigation Alerts



Keep your litigation team up-to-date with **real-time alerts** and advanced team management tools built for the enterprise, all while greatly reducing PACER spend.

Our comprehensive service means we can handle Federal, State, and Administrative courts across the country.

## Advanced Docket Research



With over 230 million records, Docket Alarm's cloud-native docket research platform finds what other services can't. Coverage includes Federal, State, plus PTAB, TTAB, ITC and NLRB decisions, all in one place.

Identify arguments that have been successful in the past with full text, pinpoint searching. Link to case law cited within any court document via Fastcase.

## Analytics At Your Fingertips



Learn what happened the last time a particular judge, opposing counsel or company faced cases similar to yours.

Advanced out-of-the-box PTAB and TTAB analytics are always at your fingertips.

## API

Docket Alarm offers a powerful API (application programming interface) to developers that want to integrate case filings into their apps.

## LAW FIRMS

Build custom dashboards for your attorneys and clients with live data direct from the court.

Automate many repetitive legal tasks like conflict checks, document management, and marketing.

## FINANCIAL INSTITUTIONS

Litigation and bankruptcy checks for companies and debtors.

## E-DISCOVERY AND LEGAL VENDORS

Sync your system to PACER to automate legal marketing.